Toxicity of CdTe Quantum Dots in Bacterial Strains

Eve-Marei Dumas, Valéry Ozenne, Randall E. Mielke, and Jay L. Nadeau*

***Abstract*—Contradictory results on quantum dot cytotoxicity exist for many types of biological systems, especially microorganisms. In this study, we compare the cytotoxicity of CdTe quantum dots (QDs) to four very different environmental bacterial strains, giving quantitative models of the growth curves for exposed organisms. The mechanisms of toxicity are explored by measuring reactive oxygen species generation by the QDs alone and investigating the oxidative damage to mutant bacteria especially sensitive to ROS. Electron microscopic examination also reveals factors that may contribute to resistance to nanoparticles in some strains.**

***Index Terms*—Bacteria, CdTe, quantum dot (QD), reactive oxygen species (ROS).**

I. Introduction

SEMICONDUCTOR nanoparticles, also called quantum dots (QDs), are desirable as an alternative to organic fluorophores due to their wide absorbance and narrow emission spectra. These properties, coupled with their low photobleaching, allow for distinctive labeling of many entities that can be excited by a single wavelength [1]–[3]. However, only recently has the cytotoxicity of these bioimaging tools been explored. Cytotoxicity of CdTe QDs has been observed in mammalian cells and bacteria [4]–[7]. Bacterial studies have been performed with other types of semiconductor nanoparticles, especially TiO_2 [8]–[11], and also ZnO [7], [12], [13] and SiO_2 [11], [14], and some comparisons of bacterial strains have been performed. With all of these particles, mechanisms of toxicity were attributed to oxidation: either the photogeneration of reactive oxygen species (ROS) by the particles or the direct release of metal ions (such as Cd^{2+}) that can cause oxidative toxicity.

However, many open questions and controversies remain. In some studies, the Gram-positive test strain was more sensitive than the Gram-negative [15]; in others, it was the opposite [16]. Because Gram-positive strains are often spore formers, the question of sporulation often complicates studies. The type of light exposure used between studies has also varied greatly, from natural sunlight [17] to high-intensity lamps [18].

Most importantly, a quantitative comparison of multiple strains of different Gram signs has never been performed. Such a model would be important and practical for several reasons. The different structures of Gram-positive and Gram-negative cell walls may affect QD binding to the bacteria, which can affect direct toxicity as well as toxicity caused by ROS. Because of the short lifetime of singlet oxygen in water, it is unlikely to diffuse to a cell surface if it is generated in solution (estimated diffusion radius: 10–20 nm) [19]. However, its lifetime may be significantly longer in cells and membranes [20], and thus, its generation from a membrane-bound particle is much more likely to cause cytotoxicity.

Direct oxidation of cell lipids and proteins may also play a role in QD-mediated cytotoxicity, as has been recently suggested for C60 [21]. Direct interaction of metal or semiconductor nanoparticles with components of the electron transport chain may allow these particles to be used as a source of energy [22], or may cause toxicity by inhibiting respiration [23]. Variations among strains are likely to be very important in these mechanisms.

In addition, the mechanisms of heavy metal resistance in Gram positives and Gram negatives are very different [24], [25]. In the case of cadmium, which is the heavy metal of interest in this study, bacterial plasmids encode for the expulsion system of toxic metal ions. Cadmium ions (Cd^{2+}) are pumped out of Gram-positive bacteria by an ATPase with a phosphoaspartate intermediate, which is encoded on a gene named *cadA*. In the case of Gram-negative bacteria, Cd^{2+} (as well as Zn^{2+}, Ni^{2+}, and Co^{2+}) are expulsed by a three-polypeptide membrane complex that functions as a divalent cation/$2H^+$ antiporter [25].

The goal of this study was to quantify the toxicity of CdTe QDs to four test strains of bacteria (two Gram-negative and two Gram-positive) as a function of the time and QD concentration. Modeling of the growth curves allowed us to determine bactericidal and bacteriostatic QD concentrations for each strain and to calculate the fraction of cells killed immediately after nanoparticle irradiation versus those that were inhibited or killed later. In order to confirm the mechanism of toxicity provided by the QDs, we ran the same assay using a mutated strain of *Escherichia coli* sensitive to oxidative stress. Electron micrographs of the exposed and unexposed bacteria revealed structural damage with and without irradiation. Finally, we used a colorimetric assay to directly measure the generation of ROS by CdTe in solution.

Manuscript received October 31, 2008. First published March 16, 2009; current version published June 24, 2009. This work was supported by the U.S. Environmental Protection Agency, the Canadian Institutes of Health Research (CIHR) Nanomedicine and Regenerative Medicine Program, and the National Science and Engineering Research Council (NSERC) Individual Discovery grant. The work of E.-M. Dumas was supported by the Townshend Foundation. *Asterisk indicates corresponding author.*

E.-M. Dumas is with the Department of Biomedical Engineering, McGill University, Montreal, QC H3A 2B4, Canada (e-mail: eve-marie.dumas@mail.mcgill.ca).

V. Ozenne was with the McGill University, Montreal, QC H3A 2B4, Canada. He is now with the Institut Polytechnique de Grenoble, 38016 Grenoble Cedex 1, France (e-mail: ozennev@minatec.inpg.fr).

R. E. Mielke is with the Jet Propulsion Laboratory, California Institute of Technology (Caltech)/NASA, Pasadena, CA 91109 USA (e-mail: rem@jpl.nasa.gov).

*J. L. Nadeau is with the Department of Biomedical Engineering, McGill University, Montreal, QC H3A 2B4, Canada (e-mail: jay.nadeau@mcill.ca).

Digital Object Identifier 10.1109/TNB.2009.2017313

1536-1241/$25.00 © 2009 IEEE

II. Materials and Methods

A. QD Synthesis and Characterization

Unless stated otherwise, all chemicals were purchased from Sigma-Aldrich Canada (Oakville, ON). The cadmium telluride QDs used were synthesized following a recently developed procedure [26]. In a few words, 0.026 g (0.20 mmol) of CdO and 0.179 g (0.63 mmol) OA were added to a three-neck flask containing 10 mL of 1-octadecene (ODE). This mix was degassed for 5 min and heated under nitrogen (N_2) to 220 °C until the solution became colorless. In a separate vessel, the tellurium precursor (trioctylphosphine telluride, TOPTe) was prepared by mixing 0.01 g (0.08 mmol) of Te with 0.415 g (1.12 mmol) trioctylphosphine (TOP) and 2 mL ODE under N_2 atmosphere and this mixture was vigorously stirred until the solution became light yellow. The temperature of the CdO–ODE mixture was further increased to 310 °C, which allowed for the formation of a grey Cd^0 precipitate after 10–20 min. Immediately after formation of this precipitate, the TOPTe precursor was rapidly injected using a needled syringe. The temperature was lowered to 270 °C for the growth of the particles. Aliquots were rapidly cooled to room temperature at the desired stage of growth [26].

B. QD Purification and Solubilization

Purification of QDs was then performed in order to separate the nanocrystals from unreacted precursors. Repeated (three) extractions with an equal amount of chloroform and methanol were performed using a separatory funnel. Unreacted CdO and oleic acid (OA) are soluble in the chloroform/methanol phase while the QDs are only soluble in the ODE phase [27]. Afterward, a large excess of ethanol was added to separate the QDs from ODE and the sample was centrifuged at 10 000 *g* for 1 min. The QDs formed a thick paste on the bottom of the centrifuge tube and toluene was added to dilute the solution to an optical density (OD) at the exciton peak of approximately 5. Aliquots were stored in the dark in airtight vials until further use.

Because of the instability of solubilized CdTe QDs, the particles were solubilized and cleaned right before their use in an experiment. In a 2-mL eppendorf tube, we placed 200 μL of the unsolubilized stock. To this tube, we successively added 800 μL of toluene (ACP Chemicals, Inc., QC), 1 mL of 200 mM borate buffer at pH 8.9, and 2 μL of 3-mercaptopropionic acid (MPA). The mixture was vortexed until the QDs had transferred from the top to the bottom phase of the tube. The tube was then spun at 17 000 *g* for 30 s in a tabletop centrifuge. The QDs were then pipetted out, carefully avoiding the nonaqueous phase, and distributed equally into two Vivaspin 500 ultrafiltration centrifugal devices with a polyethersulfone (PES) membrane and a molecular weight cutoff of 10 000 (VWR). The filters were then filled to 750 μL with 40 mM borate buffer.

The filters were spun following the manufacturer's instructions for 13 min at 2000 *g*. The QDs were then resuspended in borate buffer and the procedure was repeated three more times. The sample's concentration was then determined by measuring its absorbance at the exciton peak and estimating size and extinction coefficient according to published methods [28].

C. Bacterial Strains

Wild-type strains were purchased from American Type culture Collection (ATCC), Manassas, VA; these included two Gram-negative strains: *E. coli* ATCC 25922 and *Pseudomonas aeruginosa* ATCC 10145U, and two Gram-positive strains: *Staphylococcus aureus* ATCC 29213 and *Bacillus subtilis* ATCC 9372. The $oxyR^-$ and $oxyR^+$ strains of *E. coli* were a gift of Manuel Blanco, Centro de Investigacion Prıncipe Felipe, Valencia, Spain.

The incubation temperature was 37 °C and the growth medium used was Luria–Bertani (LB; Difco, Sparks, MD) broth for all wild-type strains and brain heart infusion (BHI; Difco) for the OxyR strains. On the eve of the experiment, for each strain, 88 μL of an existing bacterial stock, which was kept at 4 °C, was added to 5 mL of fresh medium. The tubes were incubated at 37 °C, on a shaker, for 12–18 h.

The next day, 200 μL of this new stock was placed into 10 mL of fresh medium. The bacteria were then transferred into a transparent 96-well plate (200 μL per well), which was placed into a plate reader (SpectraMax Plus, Molecular Devices) in order to measure the OD of each well at 600 nm (OD600).

The growth curves of each bacterial strain were monitored until the OD was 0.05, and then the treatments were applied (except for the OxyR strains, where treatments were applied at OD600 = 0.15). All treatments were applied in quadruplicate, and each experiment was repeated at least three times. QD samples were added to each well at concentrations reported in Section III except for a bacteria-only control, which was included in all experiments. Controls were subjected to the same conditions of light, temperature, and shaking. Irradiation was performed using a custom 440 nm 96-LED lamp for 30 min. Bacterial growth was monitored by measuring OD600 every 10 min for 4–8 h on the plate reader.

For plate counts, bacteria were treated in a 96-well plate exactly as for the time-course experiments. Immediately after irradiation, they were diluted 1 in 10^5 to 1 in 10^6 in LB medium to give control plates with $\sim$100 colonies. The bacteria were spread uniformly on LB agar plates and colonies counted by hand the following day.

D. Scanning Transmission Electron Microscopy

Scanning transmission electron microscopy (STEM) imaging was performed on an FEI Nano600 FEG scanning electron microscope (SEM). Ultrathin sections (60 nm) were made from resin-embedded samples as described [29] and placed on formvar-coated 200-mesh copper grids. A 30 kV accelerating voltage was used to image with the STEM detector at a 6.7 mm working distance.

E. XTT Assay

The XTT assay was based upon published methods [21]. In a 96-well plate, varying concentrations of solubilized and cleaned CdTe QDs were placed in dH_2O to a total volume of 100 μL. Then, 100 μM of 2,3-bis(2-methoxy-4-nitro-5-sulfophenyl)-2 H-tetrazolium-5-carboxanilide (XTT) solution was added and

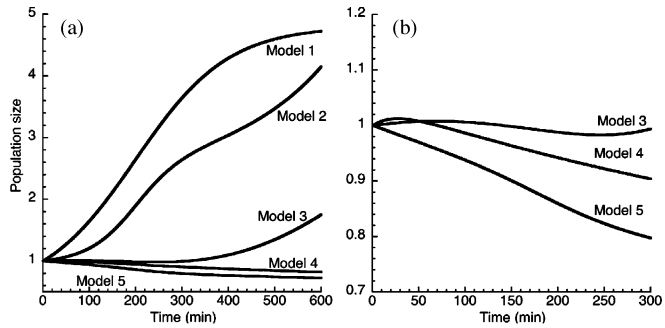

Fig. 1. Models of bacterial growth described by (1). (a) All models showing population size normalized to $t = 0$ with parameters chosen to lead to stationary behavior by ~600 min. (b) Zoom-in of early times of decaying models 4, 5, and 6 showing the differences. Note, especially the slight increase in model 4 followed by the decay. This was a commonly observed feature of our bacterial populations.

the colorimetric change monitored by absorbance at 470 nm at time 0, then every 5–10 min for 1 h after irradiation with the 440 nm lamp.

F. Data Analysis and Curve Fitting

Growth curve data were analyzed using Prism 4.0 (GraphPad Software, CA) with custom fit equations corresponding to our model.

III. Results

A. Growth Curves and Modeling

The goal of the growth curve analysis was to find a model with a minimum number of physically relevant parameters that would fit all observed situations. A general equation for a bacterial growth curve in the presence of a toxic agent can be given in terms of a fraction of cells, k_{dying}, killed by the treatment and undergoing exponential decay at a rate α; a fraction of cells, k_{stat}, prevented from reproducing but not killed outright; and a fraction of cells that continues to grow in a characteristic fashion, with a maximal growth rate β and a time to achieve half-maximum τ [30]. The sum of these three populations leads to the equation for population size x as a function of time t

$$x(t) = \frac{k - k_{\mathrm{stat}}}{1 + \exp\left[\beta(V_{50} - t)\right]} + k_{\mathrm{stat}} + k_{\mathrm{dying}} \exp(-\alpha t). \tag{1}$$

Depending upon the bacterial strain and the QD concentration, not all of these parameters were required to fit each curve. In addition, changing signs of certain parameters could be used to define new models using the same equation. For instance, if $\alpha < 0$, k_{dying} becomes $k_{\mathrm{surviving}}$ and the model describes a fraction of the surviving cells that begins to grow exponentially; i.e., cell death is limited by the amount of the toxin or the damage to the cell.

Five distinct types of curves could describe all of the observed curves. These models are illustrated in Fig. 1.

Model 1: No cell death, classic S-shaped growth curve. $k_{\mathrm{dying}} = 0$.

Model 2: Short lag followed by exponential growth. $k_{\mathrm{dying}} > 0$, $\beta > 0$.

Model 3: Long lag followed by exponential growth. $k_{\mathrm{dying}} > 0$, may have $\beta < 0$ and $\alpha < 0$.

Model 4: Slow rise followed by decay. $\alpha > 0$, $\beta > 0$, $k_{\mathrm{dying}} > k$.

Model 5: Exponential decay only. $\alpha > 0$, $k = k_{\mathrm{stat}} = 0$.

A wide variation in sensitivity to CdTe QDs was seen with the four strains. QD concentrations were varied to span a range of effects, from the first perceptible reduction in growth rate (model 2) to complete death of the population without perceptible recovery (model 4 or 5). This latter condition was not seen without irradiation; with irradiation, concentrations needed for kill ranged from 0.3 μM for *S. aureus* and *E. coli* to 0.6 μM for *B. subtilis* (Fig. 2).

The value of the model parameters' physical value could be appreciated by examining the relationship between QD concentration and the fraction f of the population that was killed, calculated as

$$f = \frac{k_{\mathrm{dying}}}{k + k_{\mathrm{dying}} + k_{\mathrm{stat}}}. \tag{2}$$

Using this formula, it could be seen that *E. coli* and *P. aeruginosa*, the Gram-negative strains, both showed a similar pattern of sudden transition to toxicity at a given QD concentration. *E. coli* was somewhat more sensitive, so that the concentration at which this occurred was lower. For example, a concentration of 0.3 mM CdTe was harmless for *P. aeruginosa* but caused significant death in *E. coli* (Fig. 3).

A similar pattern was not seen consistently with either of the Gram-positive strains. Both *B. subtilis* and *S. aureus* showed large variations in response to similar QD concentrations, e.g., f from 0 to 0.25 for 0.3 μm CdTe in four independent experiments. The bacteria alone also showed greatly varying growth curves, especially when irradiated. On two occasions, *S. aureus* grew nearly twice as fast when irradiated (not shown).

Plate counts were also performed to confirm the effects. For *E. coli*, all tested concentrations of QDs (0.04, 0.2, and 0.3 μM) gave the same results: a 78 ± 5% reduction in colony counts when irradiated ($n = 3$, as compared to irradiated controls with no QDs). This suggested that the cells that recovered at late times in medium were not capable of forming colonies, at least on LB. In contrast, there was no significant effect on *P. aeruginosa* colony counts for QD concentrations up to 0.4 μM ($n = 3$). For *B. subtilis*, a 0.6 μM QD concentration consistently led to a ~70% reduction in colony counts ($n = 3$), and either 0.2 or 0.4 μM led to a 30% reduction. As with the growth curves, the response of *S. aureus* was too variable to quantify.

B. OxyR Strains

In order to determine whether the observed cytotoxicity was mediated by ROS, we used a variant of a recently developed assay using *E. coli* mutant strains [31]–[33]. The stain IC5204 (*oxy*R$^-$) is sensitive to oxidative stress because of its deficiency

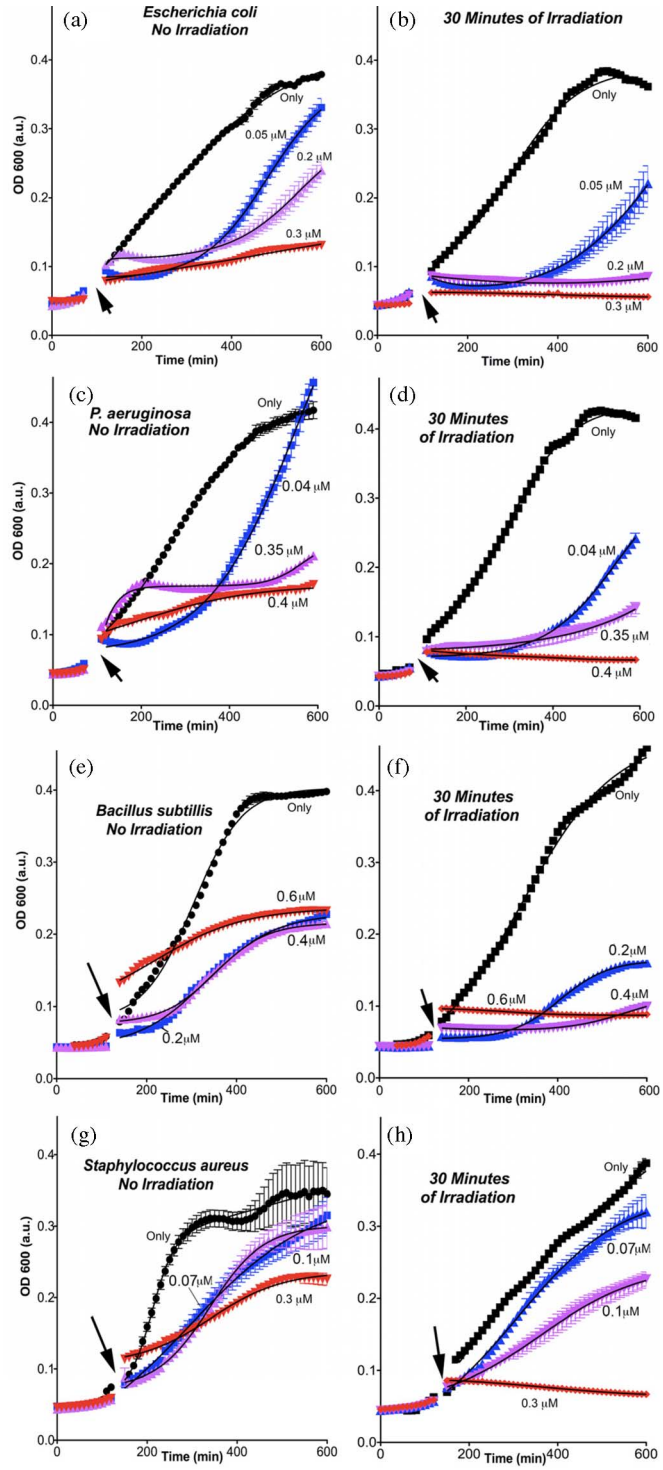

Fig. 2. Growth curves with and without irradiation for bacteria only (black) and with the indicated concentration of CdTe. The concentrations chosen represent complete population death with irradiation (model 5, red); the first perceptible effects (model 2, blue); and a value between those two concentrations that allowed for some recovery (model 3, magenta). The symbols are data points and the lines are fits to (1) with $R > 0.99$ for all fits. The arrow marks the point at which QDs were added and the samples were irradiated (nonirradiated samples were at room temperature for this period). Error bars are standard errors of quadruplicates; when they do not appear, they are smaller than the symbols.

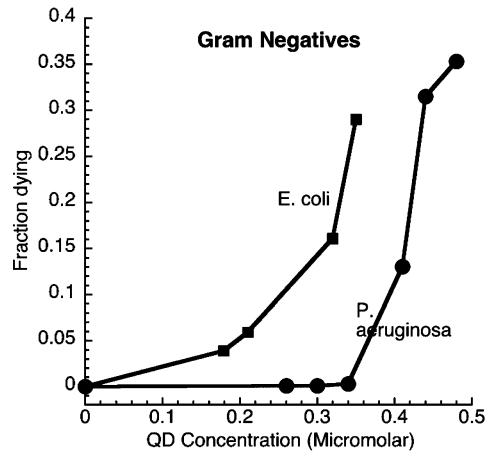

Fig. 3. Fraction dying (2) versus QD concentration for the Gram-negative strains with irradiation. Error bars are smaller than symbols for three to four experiments.

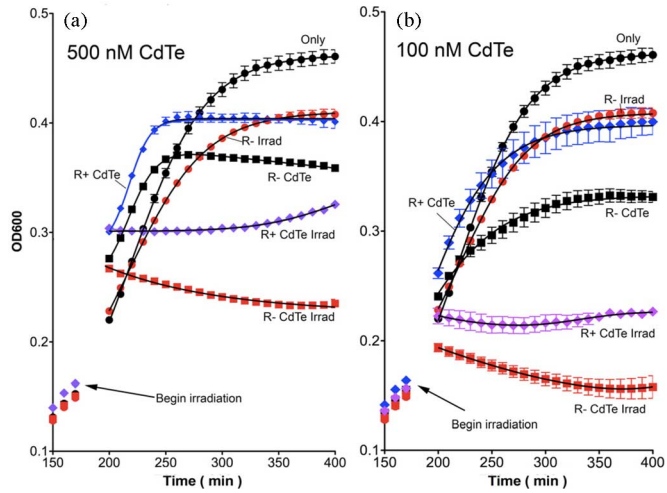

Fig. 4. Growth curves for OxyR strains. "R−" indicates the $oxyR^-$ strain, and "R+" the $oxyR^+$ strain. The "Only" refers to $oxyR^-$ only, OxyR+ only, and OxyR+ irradiated, all of which overlapped. Lines show fits as in Table I.

in the OxyR protein, a redox-sensitive transcriptional regulator that has a role in the activation of genes coding for antioxidant enzymes [31], [34], [35]. We also used IC5282 ($oxyR^+$) strain whose OxyR production remains intact as a control.

Growth curves showed significantly greater toxicity for CdTe in the $oxyR^-$ strain, even without irradiation (Fig. 4). With irradiation, 100 nM CdTe greatly inhibited the $oxyR^-$ strain [model 4, Fig. 4(b)], but only slowed the $oxyR^+$ strain (model 3). Five hundred nanomolar CdTe killed the $oxyR^-$ strain but only inhibited the $oxyR^+$ strain. The irradiation alone had a moderate effect on the $oxyR^-$ strain, reducing its growth rate significantly [Fig 4(a) and (b)]. Table I shows the fit values for concentrations at which transitions to a different model were seen for each strain.

C. STEM

STEM allows for imaging ultrathin slices of bacteria, showing nanoparticle internalization and allowing for visualization of the

TABLE I
FIT PARAMETERS FOR OXYR STRAINS

	k	k_{stat}	k_{dying}	β	V_{50}	α	Model
R-	0.462	0.082	0	0.03	219	0	1
100 nM	0.332	0.032	0	0.02	164	0	1
500 nM	0.132	0	0.274	0.08	217	0.0005	4
Rad	0.137	0.052	0	0.02	337	0	1
Rad 100 nM	0.164	0.088	0.208	0.03	451	0.0034	4
Rad 500 nM	0	0	0.316	0	0	0.0009	5
R+	0.071	0	0	0.04	174	0	1
500 nM	0.403	0.287	0	0.10	218	0	1
Rad	0.182	0.033	0	0.02	221	0	1
Rad 100 nM	0.226	0.205	0.255	0.04	327	0.0132	3
Rad 500 nM	0.354	0.300	3397	0.03	404	0.069	3

*The top six rows apply to $oxyR^+$ with the concentration of CdTe indicated in nanomolar and "Rad" to mean irradiation. The bottom five values are the $oxyR^+$ strain. Concentrations show reflects where changes in toxicity were seen; note that model 5 (death only) was only seen with the $oxyR^+$ strain.

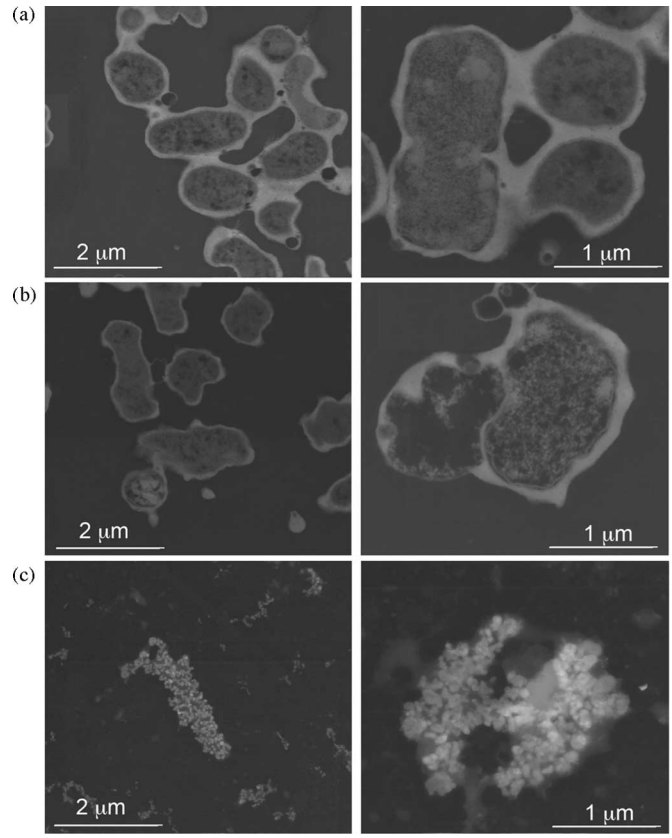

Fig. 5. STEM images of $oxyR^-$ cells exposed to CdTe QDs. (a) Untreated cells. Note intracellular texture and abundant EPS. (b) Cells exposed to 500 nM CdTe without irradiation. Note thinning of EPS layer; some membrane blebbing is apparent in the right-hand panel. The smaller cell on the left, which appears empty, is dead. (c) Cells exposed to 500 nM CdTe with 30 min blue light irradiation. No cells can be distinguished.

cell contents [36]. Using this technique, we were able to observe the CdTe toxicity to the $oxyR^-$ strain before and after irradiation. Compared to untreated cells [Fig. 5(a)], CdTe-exposed cells showed a distinct thinning of the exopolysaccharide (EPS) layer. Internalization of nanoparticles could be seen, often to a very large extent, and some cells showed membrane blebbing or complete emptiness of the cytoplasmic cavity [Fig. 5(b)]. After irradiation, no intact cells were seen, but only fragments and clusters of nanoparticles [Fig. 5(c)].

D. XTT Assay

XTT provides a colorimetric signal when reduced by superoxides (O_2^-). It is a more reliable test for ROS generation from nanoparticles than oxidation-based dyes such as 5-(and-6)-carboxy-2′,7′-dichlorodihydrofluorescein or dihydroethidium, as such probes may be directly oxidized by nanoparticles without necessarily creating an ROS intermediate [21]. Using this assay, we found a clear signal with CdTe that was dependent upon QD concentration and light exposure (Fig. 6).

IV. DISCUSSION

The kinetic model that we used has been used previously to describe toxicity to *Listeria monocytogenes*. The five parameters in the model correspond to physical values; exponential decay of the dying fraction gives better fits than a second Boltzmann [30]. We took the analysis one step further by defining five distinct behaviors of the equation, defined as one or more of the parameters go to zero or change sign. This allows for a rapid identification of thresholds of toxicity of an antibacterial agent.

Use of this model yielded a concentration versus toxicity curve for the Gram-negative strains, which showed a nearly all-or-nothing kill rate and slightly more resistance to toxicity with *P. aeruginosa* over *E. coli*. This latter result is not surprising, as the thick EPS layer of *P. aeruginosa* can prevent QD binding. The EPS may also protect against ROS as has been found in plant pathogenic strains of *Pseudomonas* [37].

The results for the Gram-positive strains were less clear. *B. subtilis* showed the highest concentration required to kill all of the cells, but the toxicity values at intermediate concentrations varied widely. We believe that the "kill" value is real and not an artefact of sporulation, as we could observe sporulation as a sudden drop in OD600. The intermediate-concentration effects on *S. aureus*, a nonspore former, were equally scattered, suggesting that sporulation did not play a major role in these conflicting results. One possible confounding factor is the light itself, which had an unpredictable effect on *S. aureus*, sometimes stimulating its growth.

Plate counts indicated that *E. coli* cells that recovered late were unable to form colonies. The opposite effect was seen with *B. subtilis*, where a growth curve indicating 100% kill still yielded colonies when plated. This result is certainly due to the formation of *B. subtilis* endospores, which could be observed

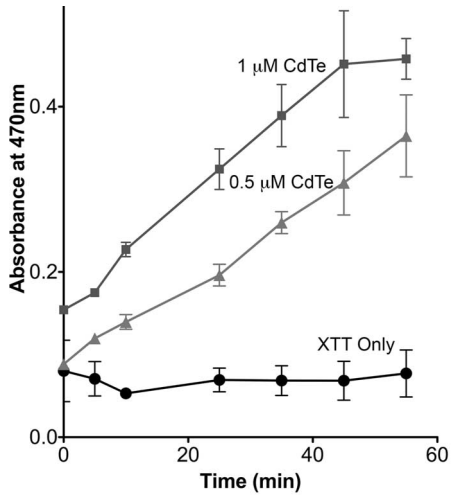

Fig. 6. Results of XTT assay (absorbance at 470 nm) for two concentrations of QDs and an XTT-only control under blue light irradiation. The data points are means of three experiments, each done in quadruplicate, and the error bars are SEM.

in the treated cultures (not shown). *P. aeruginosa* plate counts indicated significant resistance of this strain to QDs.

The results with the OxyR strains were consistent with previous reports showing that CdTe toxicity to *E. coli* is mediated by oxidative stress and influences the expression of antioxidant enzymes [38]. Very low levels of CdTe were required to completely kill the $oxyR^-$ strain. The $oxyR^+$ strain, which differs only in a single oxidative gene, is resistant to up to 100-fold more CdTe. Cell damage and death can be observed even before irradiation, probably due to the release of free Cd^{2+} ions. With irradiation, $oxyR^-$ cells are entirely destroyed in the presence of CdTe.

Reports of ROS generation from QDs have been difficult to interpret, in a large part because most ROS indicators become colorimetric or fluorescent when oxidized. However, they can be directly oxidized by nanoparticles rather than through the intermediary of ROS. A recent report found that C60, previously believed to release ROS, showed no signal with the XTT assay, which is based upon reduction rather than oxidation [21]. Using this assay, we found a concentration- and light-dependent colorimetric effect, suggesting that CdTe QDs do, in fact, generate superoxide in aqueous solution.

V. Conclusion

Of our four environmental strains, *B. subtilis* is the most resistant to CdTe and *P. aeruginosa* is more resistant than *E. coli*. However, the Gram-positive strains showed a lack of reproducibility, and effects of light on the strains should be considered in future studies. Toxicity is mediated through ROS.

References

[1] W. C. Chan, D. J. Maxwell, X. Gao, R. E. Bailey, M. Han, and S. Nie, "Luminescent quantum dots for multiplexed biological detection and imaging," *Curr. Opin. Biotechnol.*, vol. 13, pp. 40–46, 2002.

[2] W. C. Chan and S. Nie, "Quantum dot bioconjugates for ultrasensitive nonisotopic detection," *Science*, vol. 281, pp. 2016–2018, Sep. 25, 1998.

[3] T. M. Jovin, "Quantum dots finally come of age," *Nature Biotechnol.*, vol. 21, pp. 32–33, Jan. 2003.

[4] S. J. Cho, D. Maysinger, M. Jain, B. Roder, S. Hackbarth, and F. M. Winnik, "Long-term exposure to CdTe quantum dots causes functional impairments in live cells," *Langmuir*, vol. 23, pp. 1974–1980, Feb. 13, 2007.

[5] C. Kirchner, A. M. Javier, A. S. Susha, A. L. Rogach, O. Kreft, G. B. Sukhorukov, and W. J. Parak, "Cytotoxicity of nanoparticle-loaded polymer capsules," *Talanta*, vol. 67, pp. 486–491, Sep. 2005.

[6] J. Lovric, H. S. Bazzi, Y. Cuie, G. R. Fortin, F. M. Winnik, and D. Maysinger, "Differences in subcellular distribution and toxicity of green and red emitting CdTe quantum dots," *J. Mol. Med.*, vol. 83, pp. 377–385, May 2005.

[7] H. Yang, C. Liu, D. Yang, H. Zhang, and Z. Xi, "Comparative study of cytotoxicity, oxidative stress and genotoxicity induced by four typical nanomaterials: the role of particle size, shape and composition," *J. Appl. Toxicol.*, vol. 29, no. 1, pp. 69–78, Aug. 29, 2008.

[8] R. Cai, Y. Kubota, T. Shuin, H. Sakai, K. Hashimoto, and A. Fujishima, "Induction of cytotoxicity by photoexcited TiO2 particles," *Cancer Res.*, vol. 52, pp. 2346–2348, Apr. 15, 1992.

[9] C. Y. Jin, B. S. Zhu, X. F. Wang, and Q. H. Lu, "Cytotoxicity of titanium dioxide nanoparticles in mouse fibroblast cells," *Chem. Res. Toxicol*, vol. 21, pp. 1871–1877, Sep. 2008.

[10] W. F. Vevers and A. N. Jha, "Genotoxic and cytotoxic potential of titanium dioxide (TiO2) nanoparticles on fish cells in vitro," *Ecotoxicology*, vol. 17, pp. 410–420, Jul. 2008.

[11] J. J. Wang, B. J. Sanderson, and H. Wang, "Cyto- and genotoxicity of ultrafine TiO2 particles in cultured human lymphoblastoid cells," *Mutatgen Res.*, vol. 628, pp. 99–106, Apr. 2, 2007.

[12] D. Guo, C. Wu, H. Jiang, Q. Li, X. Wang, and B. Chen, "Synergistic cytotoxic effect of different sized ZnO nanoparticles and daunorubicin against leukemia cancer cells under UV irradiation," *J. Photochem. Photobiol. B*, vol. 93, pp. 119–126, Aug. 8, 2008.

[13] S. Nair, A. Sasidharan, V. V. Divya Rani, D. Menon, K. Manzoor, and S. Raina, "Role of size scale of ZnO nanoparticles and microparticles on toxicity toward bacteria and osteoblast cancer cells," *J. Mater. Sci. Mater. Med.*, to be published.

[14] W. Lin, Y. W. Huang, X. D. Zhou, and Y. Ma, "In vitro toxicity of silica nanoparticles in human lung cancer cells," *Toxicol Appl. Pharmacol.*, vol. 217, pp. 252–259, Dec. 15, 2006.

[15] G. Fu, P. S. Vary, and C. T. Lin, "Anatase TiO2 nanocomposites for antimicrobial coatings," *J. Phys. Chem. B*, vol. 109, pp. 8889–8898, May 12, 2005.

[16] A. G. Rincon and C. Pulgarin, "Use of coaxial photocatalytic reactor (CAPHORE) in the TiO2 photo-assisted treatment of mixed *Escherichia coli* and *Bacillus subtilis* and the bacterial community present in wastewater," *Catal. Today*, vol. 101, pp. 331–344, 2005.

[17] L. K. Adams, D. Y. Lyon, and P. J. Alvarez, "Comparative eco-toxicity of nanoscale TiO2, SiO2, and ZnO water suspensions," *Water Res.*, vol. 40, pp. 3527–3532, Nov. 2006.

[18] P. C. Maness, S. Smolinski, D. M. Blake, Z. Huang, E. J. Wolfrum, and W. A. Jacoby, "Bactericidal activity of photocatalytic TiO(2) reaction: toward an understanding of its killing mechanism," *Appl. Environ. Microbiol.*, vol. 65, pp. 4094–4098, Sep. 1999.

[19] R. W. Redmond and I. E. Kochevar, "Spatially resolved cellular responses to singlet oxygen," *Photochem. Photobiol.*, vol. 82, pp. 1178–1186, Sep./Oct. 2006.

[20] E. Skovsen, J. W. Snyder, J. D. Lambert, and P. R. Ogilby, "Lifetime and diffusion of singlet oxygen in a cell," *J. Phys. Chem. B*, vol. 109, pp. 8570–8573, May 12, 2005.

[21] D. Y. Lyon, L. Brunet, G. W. Hinkal, M. R. Wiesner, and P. J. Alvarez, "Antibacterial activity of fullerene water suspensions (nC60) is not due to ROS-mediated damage," *Nano Lett.*, vol. 8, pp. 1539–1543, May 2008.

[22] O. Bretschger, A. Obraztsova, C. A. Sturm, I. S. Chang, Y. A. Gorby, S. B. Reed, D. E. Culley, C. L. Reardon, S. Barua, M. F. Romine, J. Zhou, A. S. Beliaev, R. Bouhenni, D. Saffarini, F. Mansfeld, B. H. Kim, J. K. Fredrickson, and K. H. Nealson, "Current production and metal oxide reduction by Shewanella oneidensis MR-1 wild type and mutants," *Appl. Environ. Microbiol.*, vol. 73, pp. 7003–7012, Nov. 2007.

[23] T. Mashino, N. Usui, K. Okuda, T. Hirota, and M. Mochizuki, "Respiratory chain inhibition by fullerene derivatives: hydrogen peroxide production caused by fullerene derivatives and a respiratory chain system," *Bioorg. Med. Chem.*, vol. 11, pp. 1433–1438, Apr. 3, 2003.

[24] D. H. Nies, "Resistance to cadmium, cobalt, zinc, and nickel in microbes," *Plasmid*, vol. 27, pp. 17–28, Jan. 1992.

[25] S. Silver, "Bacterial resistances to toxic metal ions–a review," *Gene*, vol. 179, pp. 9–19, Nov. 7, 1996.
[26] V. Kloper, R. Osovsky, J. Kolny-Olesiak, A. Sashchiuk, and E. Lifshitz, "The growth of colloidal cadmium telluride nanocrystal quantum dots in the presence of Cd-0 nanoparticles," *J. Phys. Chem. C*, vol. 111, pp. 10336–10341, Jul. 2007.
[27] W. W. Yu and X. Peng, "Formation of high-quality CdS and other II-VI semiconductor nanocrystals in noncoordinating solvents: tunable reactivity of monomers," *Angew Chem. Int. Ed. Engl.*, vol. 41, pp. 2368–2371, Jul. 2, 2002.
[28] W. W. Yu, L. H. Qu, W. Z. Guo, and X. G. Peng, "Experimental determination of the extinction coefficient of CdTe, CdSe, and CdS nanocrystals," *Chem. Mater.*, vol. 15, pp. 2854–2860, 2003.
[29] D. P. Lies, M. E. Hernandez, A. Kappler, R. E. Mielke, J. A. Gralnick, and D. K. Newman, "Shewanella oneidensis MR-1 uses overlapping pathways for iron reduction at a distance and by direct contact under conditions relevant for Biofilms," *Appl. Environ. Microbiol.*, vol. 71, pp. 4414–4426, Aug. 2005.
[30] K. M. Pruitt and D. N. Kamau, "Mathematical models of bacterial growth, inhibition and death under combined stress conditions," *J. Ind. Microbiol.*, vol. 12, pp. 221–231, 1993.
[31] A. Urios, M. Largeron, M. B. Fleury, and M. Blanco, "A convenient approach for evaluating the toxicity profiles of in vitro neuroprotective alkylaminophenol derivatives," *Free Radic. Biol. Med.*, vol. 40, pp. 791–800, Mar. 1, 2006.
[32] A. Martinez, A. Urios, and M. Blanco, "Mutagenicity of 80 chemicals in *Escherichia coli* tester strains IC203, deficient in OxyR, and its oxyR(+) parent WP2 uvrA/pKM101: Detection of 31 oxidative mutagens," *Mutat. Res.*, vol. 467, pp. 41–53, Apr. 13, 2000.
[33] A. Urios, M. P. Lopez-Gresa, M. C. Gonzalez, J. Primo, A. Martinez, G. Herrera, J. C. Escudero, J. E. O'Connor, and M. Blanco, "Nitric oxide promotes strong cytotoxicity of phenolic compounds against *Escherichia coli:* The influence of antioxidant defenses," *Free Radic. Biol. Med.*, vol. 35, pp. 1373–1381, Dec. 1, 2003.
[34] M. F. Christman, R. W. Morgan, F. S. Jacobson, and B. N. Ames, "Positive control of a regulon for defenses against oxidative stress and some heat-shock proteins in *Salmonella typhimurium*," *Cell*, vol. 41, pp. 753–762, Jul. 1985.
[35] M. Zheng, X. Wang, L. J. Templeton, D. R. Smulski, R. A. LaRossa, and G. Storz, "DNA microarray-mediated transcriptional profiling of the *Escherichia coli* response to hydrogen peroxide," *J. Bacteriol.*, vol. 183, pp. 4562–4570, Aug. 2001.
[36] J. R. Morones, J. L. Elechiguerra, A. Camacho, K. Holt, J. B. Kouri, J. T. Ramirez, and M. J. Yacaman, "The bactericidal effect of silver nanoparticles," *Nanotechnology*, vol. 16, pp. 2346–2353, Oct. 2005.
[37] Z. Kiraly, H. M. El-Zahaby, and Z. Klement, "Role of extracellular polysaccharide (EPS) slime of plant pathogenic bacteria in protecting cells to reactive oxygen species," *J. Phytopathol.*, vol. 145, pp. 59–68, 2008.
[38] Z. Lu, C. M. Li, H. Bao, Y. Qiao, Y. Toh, and X. Yang, "Mechanism of antimicrobial activity of CdTe quantum dots," *Langmuir*, vol. 24, pp. 5445–5452, May 20, 2008.

Eve-Marei Dumas is currently working toward the Master's degree biomedical engineering at McGill University, Montreal, QC, Canada, where she is engaged in the cytotoxity of quantum dots in both prokaryotes and eukaryotes.

Valéry Ozenne is currently working toward the Master's degree in physics from the École normale supérieure (ENS), Paris, France.

In 2008, he was an Intern at McGill University, Montreal, QC, Canada.

Randall E. Mielke has been an engineer at the Jet Propulsion Laboratory, California Institute of Technology (Caltech)/NASA, Pasadena, for 7.5 years. For 3 years, he was a microscopist at the University of California, Santa Barbara. He has extensive experience using various electron microscopy techniques including environmental scanning electron microscopy (ESEM), scanning transmission electron microscopy (STEM), SEM, and TEM.

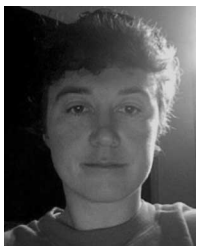

Jay L. Nadeau received the Ph.D. degree in physics from the University of Minnesota, Minneapolis, in 1996.

She was with the Astrobiology Group, Jet Propulsion Laboratory, and a Postdoctoral Fellow in the Laboratory of Henry Lester, Caltech. For the past five years, she has been a Professor of biomedical engineering, physics, and microbiology at McGill University, Montreal, QC, Canada.